2-[fluorine-18]-fluoro-2-deoxy-D-glucose: variations with body weight and a method for correction. *Radiology* 1993;189:847–850.
8. Wahl RL, Quint LE, Greenough RL, Meyer CR, White RI, Orringer MB. Staging of mediastinal non-small cell lung cancer with FDG PET, CT, and fusion images: preliminary prospective evaluation. *Radiology* 1994;191:371–377.
9. Wahl RL, Zasadny K, Greenough R, Koeppe RA. Parametric image displays to enhance visualization of cancers with FDG-PET: influx constant and temporal subtraction imaging. *77th Scientific Assembly and Annual Meeting of the Radiological Society of North America* 1991;181(suppl):152.
10. Wahl RL, Zasadny K, Helvie M, Hutchins GD, Weber B, Cody R. Metabolic monitoring of breast cancer chemohormonotherapy using positron emission tomography: initial evaluation. *J Clin Oncol* 1993;11:2101–2111.
11. Sokoloff L, Reivich M, Kennedy C, et al. The [^{14}C]deoxyglucose method for the measurement of local cerebral glucose utilization: theory, procedure, and normal values in the conscious and anesthetized albino rat. *J Neurochem* 1977;28:897–916.
12. Weber G. Enzymology of cancer cells (second of two parts). *N Engl J Med* 1977;296:541–551.
13. Bevington PR. *Data reduction and error analysis for the physical sciences*. New York: McGraw-Hill; 1992:92–133.

Noninvasive Quantification of Iodine-123-Iomazenil SPECT

Yoshihiro Onishi, Yoshiharu Yonekura, Sadahiko Nishizawa, Fumiko Tanaka, Hidehiko Okazawa, Koichi Ishizu, Toru Fujita, Junji Konishi and Takao Mukai

Nihon Medi-Physics Co., Ltd., Nishinomiya; Fukui Medical School, Fukui; Kyoto University School of Medicine, Kyoto; and Kyoto College of Medical Technology, Kyoto, Japan

The feasibility of a noninvasive method for quantification of [^{123}I]iomazenil binding using a standardized arterial input function and a single venous blood sample was assessed in normal volunteers. **Methods:** Serial SPECT images and blood data from six healthy male volunteers after intravenous injection of [^{123}I]iomazenil were used. The standardized input function was derived by averaging the six subjects' arterial curves. Individual input functions were estimated by calibrating the standardized input function with one-point venous blood radioactivity concentration. Ligand transport (K_1) and receptor binding were computed from the estimated input functions and two separate SPECT scans using a table look-up procedure based on a three-compartment, two-parameter model. Reference values for K_1 and receptor binding were determined from the serial SPECT data and individual arterial curves using a three-compartment, three-parameter model and curve fitting. **Results:** Analyses of the error caused by the calibration in relation to the time postinjection revealed that the optimal calibration time was 30 min postinjection. Receptor binding obtained by this simplified method correlated well with the reference values (r = 0.941) and was estimated within an error of 10% in the cerebral cortical regions. Although the estimated K_1 showed relatively poor correlation (r = 0.699) with the reference value, it was an excellent relative measure in each subject. **Conclusion:** Our method provided an absolute measure of the benzodiazepine receptor binding and a relative measure of ligand transport from two SPECT scans and a venous blood sample. This method would be useful for quantitative assessment of benzodiazepine receptors in clinical settings.

Key Words: iodine-123-iomazenil; standardized arterial input function; benzodiazepine receptor; SPECT

J Nucl Med 1996; 37:374–378

Iodine-123-iomazenil is a radioiodinated ligand which has favorable characteristics for in vivo assessment of benzodiazepine receptors by SPECT: high brain uptake, little nonspecific binding, high affinity for benzodiazepine receptors and no intrinsic pharmacological effects at tracer doses (*1–6*). Various SPECT studies have demonstrated the clinical feasibility of [^{123}I]iomazenil for the assessment of benzodiazepine receptors in the living human brain (*7–12*).

Brain tissue distribution of [^{123}I]iomazenil is determined by at least two independent factors, i.e., the ligand transport and the binding characteristics of the receptors. Consequently, SPECT image counts depend not only on the characteristics of the benzodiazepine receptors but also on regional cerebral blood flow, even though imaging is performed at an appropriate time after injection of the radioactive ligand. These two factors can be determined separately with SPECT or PET by using compartmental analysis (*13–19*). Quantification requirements, such as rapid serial data acquisition over a long time period and frequent arterial blood sampling, are too laborious for routine clinical practice.

Since [^{123}I]iomazenil can be used in many nuclear medicine facilities with SPECT, a noninvasive method for quantitative measurement of receptor binding would have significant clinical value. We recently demonstrated that quantification of the ligand transport and benzodiazepine receptor binding of [^{123}I]iomazenil can be achieved with two separate SPECT scans using a three-compartment, two-parameter model and a table look-up procedure (*16*). Application of such quantitative measurement would become possible in routine clinical studies if arterial blood sampling were not necessary. In this study, we used data obtained in normal volunteers to assess the precision of measures of receptor binding and ligand transport of [^{123}I]iomazenil with a single venous blood sample instead of frequent arterial blood sampling, using the concept of standardized arterial input function (*20–22*).

METHODS

Subjects

Serial SPECT images and blood data obtained in our facility for six healthy male volunteers (aged 24–61 yr; weight: 53–79 kg) after an intravenous bolus injection of 111 MBq [^{123}I]iomazenil were used (*16*). The data were acquired and processed as follows.

Blood Data. Arterial blood samples (1–3 ml) were drawn through a radial artery catheter at 5-sec intervals for the first 40 sec and subsequently at 50 sec and 1, 1.5, 2, 3, 5, 10, 20, 30, 60 and 120 min postinjection. Total radioactivity concentrations in the whole blood and plasma were measured. The lipophilic radioactivity concentration in arterial plasma was determined by chloroform extraction, followed by washing of the organic layer with saline to minimize contamination by hydrophilic metabolites (*16*). Venous blood samples were drawn at 3, 5, 10, 20, 30, 60 and 120 min after

Received Dec. 29, 1994; revision accepted Jul. 30, 1995.

For correspondence or reprints contact: Yoshihiro Onishi, Nihon Medi-Physics Co., Ltd., 9-8 Rokutanji-cho, Nishinomiya 662, Japan.

TABLE 1
SPECT Acquisition and Reconstruction Parameters

SPECT acquisition	
Type of collimators	High-resolution fan-beam*
Photowindow	159 keV ± 10%
Acquisition mode	Continuous rotating mode
Number of angular projections	120 per acquisition
Duration of each acquisition	1 min†
Total number of acquisitions	120/120 min
SPECT reconstruction	
Reconstruction algorithm	Filtered backprojection
Reconstruction filter	Butterworth filter‡
Matrix size	64 × 64
Pixel size	4.5 mm × 4.5 mm
Slice thickness	7.1 mm
Attenuation correction coefficient	0.06 cm^{-1}§
Scatter correction	None

*System spatial resolution: 3.4 mm FWHM at the surface of the collimators.

†Typical total counts for each SPECT acquisition were 200K–300K.

‡Cutoff frequency = 0.56 cm^{-1} (0.25 cycle/pixel), power factor = 4.

§The coefficient was empirically derived as the profile curves of reconstructed images of a cylindrical phantom were flat.

injection from the cubital vein, and the total radioactivity concentration in the whole blood was measured.

SPECT. SPECT images were acquired every minute until 120 min postinjection using a triple-head rotating gamma camera. SPECT acquisition and reconstruction parameters are listed in Table 1. The raw projection data were added to make a total of 27 images (ten 2-min, nine 4-min and eight 8-min images). Attenuation correction was performed by assuming uniform attenuation in the head and elliptical outline of the head based on an isodensity contour line in each slice. A calibration coefficient of 29.16 cpm/kBq for the SPECT system was derived by measuring a 16-cm diameter cylindrical phantom filled with 12 kBq/ml of ^{123}I, with the same acquisition and reconstruction procedure described above. The linearity of the SPECT system was confirmed by using different ^{123}I concentrations.

For the table look-up parameter estimation (see below), the SPECT images were added to make two 16-min images with midtimes of 12 min (early scan) and 112 min (late scan) postinjection. These corresponded to the earliest image, exclusive of the initial phase with progressively increasing SPECT counts, and the latest image within this study period, respectively. Regions of interest (ROIs) were placed on five cortical regions, and the thalamus, striatum, cerebellum and white matter/ventricle (Fig. 1).

Compartmental Model

A three-compartment model (Fig. 2) was used for parameter estimation. The mathematical solutions of the compartmental model have been previously described (*13,14,17*). The ligand concentration in each compartment is given by:

$$\frac{dC_2(t)}{dt} = K_1Ca(t) - (k_2 + k_3)C_2(t) + k_4C_3(t), \quad \text{Eq. 1}$$

$$\frac{dC_3(t)}{dt} = k_3C_2(t) - k_4C_3(t), \quad \text{Eq. 2}$$

and some kinetic parameters are defined as follows:

$$V_2 = \frac{K_1}{k_2f_1}, \quad \text{Eq. 3}$$

$$BP = \frac{K_1k_3}{k_2k_4f_1}, \quad \text{Eq. 4}$$

where Ca(t) represents the concentration of parent iomazenil in the arterial plasma compartment, $C_2(t)$ that in the free and nonspecific binding compartment, $C_3(t)$ that in the specific binding compartment, K_1–k_4 at the rate constants, f_1 the free fraction of iomazenil in the plasma, V_2 the nondisplaceable distribution volume and BP (unit: ml/ml) the "binding potential" determined as B_{max}/K_D (*23*). A fixed f_1 value of 0.24 was used throughout this study (*16*).

Two different configurations were used. One was a three-parameter configuration used with least square curve fitting to determine reference values for K_1 and BP: a constant V_2 value (K_1/k_2 = 3.0) was assumed to increase the accuracy of curve-fitting (*13,16,17*). Thus, the adjustable parameters were K_1, k_3 and k_4. The fixed K_1/k_2 ratio was derived from the results of unconstrained four-parameter fitting as previously reported (*16*) and was compatible with a value of 3.2 measured by a displacement study in an equilibrium state (*14*). The other was a two-parameter configuration used with a table look-up procedure for the estimation of K_1 and BP: k_4 was assumed as a constant in addition to fixation of the K_1/k_2 ratio. Thus, the adjustable parameters were K_1 and k_3. A fixed value of 0.026 for k_4 was derived as the average of the values obtained using the three-parameter configuration in all the cortical regions (*16*), which was not very different from the value of 0.021 reported by other investigators for the normal occipital cortexes (*15*).

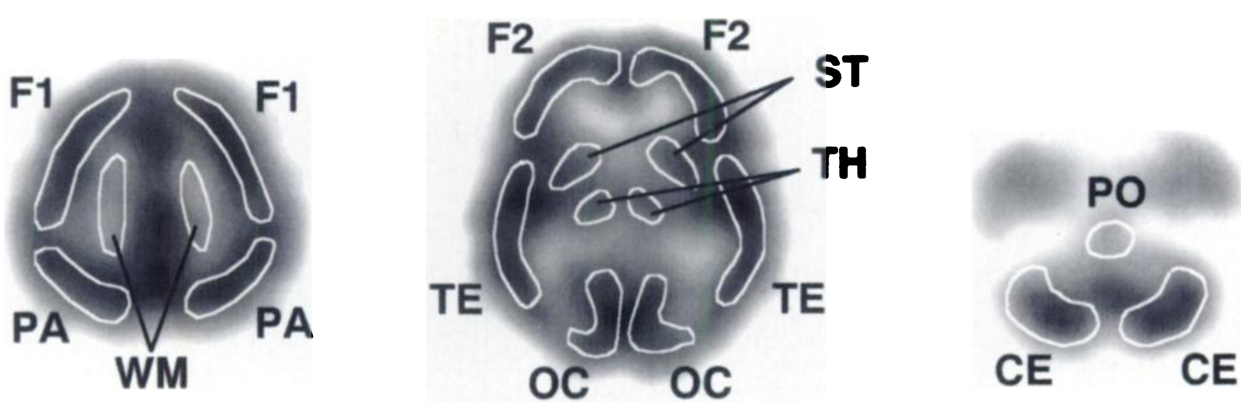

FIGURE 1. ROIs were outlined in three representative SPECT images corresponding to the level of the centrum semiovale (left), basal ganglia (middle) and cerebellum (right) on the frontal cortex (F1 and F2), parietal cortex (PA), temporal cortex (TE), occipital cortex (OC), striatum (ST), thalamus (TH), cerebellum (CE), white matter/ventricle (WM) and pons (PO). The average ROI counts of the left and right hemispheres in each region were used for the analysis (except for the pons).

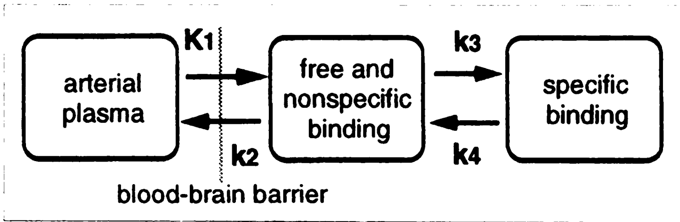

FIGURE 2. Three-compartment model. The model consists of the arterial plasma, free and nonspecific binding and specific binding compartments. K_1 (unit: ml/min/ml) and k_2–k_4 (unit: ml^{-1}) are the rate constants describing the ligand exchange between compartments. K_1/k_2 ratio was fixed to be 3.00 in the 3-parameter configuration, and k_4 was additionally fixed to be 0.026 in the two-parameter configuration.

Arterial Input Functions

Actual Input Functions and a Standardized Input Function. An actual input function (AIF) was obtained for each subject by numerical interpolation of the measured lipophilic radioactivity concentration in the arterial plasma over time. A standard shape for the arterial curve (standardized input function, SIF) was derived by averaging the six subjects' AIFs (Fig. 3).

Estimation of Arterial Plasma Lipophilic Concentration. An estimate of the lipophilic radioactivity concentration in the arterial plasma at a certain time τ ($Ca^*(\tau)$) was determined from the total radioactivity concentration in venous blood ($Cv(\tau)$) as follows:

$$Ca^*(\tau) = Cv(\tau) \times AVR(\tau) \times PBR(\tau) \times LTR(\tau), \quad \text{Eq. 5}$$

where AVR is the arterial-to-venous blood ratio of the total radioactivity concentration, PBR is the arterial plasma-to-blood ratio of the total radioactivity concentration and LTR is the lipophilic-to-total radioactivity concentration ratio in the arterial plasma (chloroform extraction ratio). The values of AVR, PBR and LTR were considered to be constant among the subjects, and the average values for the six subjects were used.

Estimated Input Functions. Estimated input function (EIF) was determined by scaling the SIF with a single lipophilic radioactivity concentration in the arterial plasma at a certain time for each subject (the term "calibrate" will be used for this operation below). Two series of EIF were determined: (a) EIF calibrated with the measured lipophilic radioactivity concentration $Ca(\tau)$ (EIF-A) and (b) EIF calibrated with the estimated lipophilic radioactivity concentration $Ca^*(\tau)$ (EIF-V), where τ represents the calibration time. In both series, the EIF was given by:

$$C_{EST}(t) = C_{STD}(t) \cdot \frac{Ca^{\circ}(\tau)}{C_{STD}(\tau)}, \quad \text{Eq. 6}$$

where $C_{EST}(t)$ and $C_{STD}(t)$ represent the EIF and SIF, respectively, $Ca^{\circ}(\tau)$ is the measured or estimated lipophilic radioactivity concentration ($Ca(\tau)$ or $Ca^*(\tau)$), and $C_{STD}(\tau)$ is the value of the SIF at time τ.

The EIF-As were used to evaluate the error caused by variation in the shape of the input functions alone, in relation to the calibration time: the differences in the area under the curve between of the AIFs and EIF-As from 0 to 10, 30, 60 and 120 min were calculated for calibration times of 10, 20, 30, 60 and 120 min postinjection. The optimal time for the calibration was determined by considering the error caused by the variation in the shape of the input functions, AVR, PBR, LTR and other practical factors. The EIF-Vs were used for the final parameter estimation by the table look-up procedure (see below).

Determining Kinetic Parameters

Reference Kinetic Parameters. The reference values of K_1 and BP were determined from the AIFs and ROI data for all 27 SPECT images (until 120 min postinjection) using the curve-fitting procedure with the three-parameter configuration.

Estimation of Kinetic Parameters by a Simplified Method. The K_1 and BP were estimated from EIF-Vs and two separate SPECT images (midtimes of 12 and 112 min postinjection) using the table look-up procedure with the two-parameter configuration. Brain tissue radioactivity concentrations in the early and late scans, B_E and B_L, are given by:

$$B_E = \int_{T_{E1}}^{T_{E2}} \int_0^t C_{EST}(s) f(t-s)\, ds dt, \quad \text{Eq. 7}$$

$$B_L = \int_{T_{L1}}^{T_{L2}} \int_0^t C_{EST}(s) f(t-s)\, ds dt, \quad \text{Eq. 8}$$

respectively, where T_{E1} and T_{E2} are the start and end times of the early scan. T_{L1} and T_{L2} are those of the late scan and f(t) is the transfer function derived from Equations 1 and 2. Inserting Equation 6 ($Ca^{\circ}(\tau) = Ca^*(\tau)$ for the use of EIF-V) into Equation 7 and into Equation 8 divided by Equation 7 gives

$$B_E \cdot \frac{C_{STD}(\tau)}{Ca^*(\tau)} = \int_{T_{E1}}^{T_{E2}} \int_0^t C_{STD}(s) f(t-s)\, ds dt, \quad \text{Eq. 9}$$

$$\frac{B_L}{B_E} = \frac{\int_{T_{L1}}^{T_{L2}} \int_0^t C_{STD}(s) f(t-s)\, ds dt}{\int_{T_{E1}}^{T_{E2}} \int_0^t C_{STD}(s) f(t-s)\, ds dt}. \quad \text{Eq. 10}$$

Since the above simultaneous equations cannot be solved analytically for the objective parameters K_1 and k_3 which are contained in $f(t)$, a table look-up procedure was used to determine the parameters from the SPECT counts: first, possible sets of $B_E \cdot (C_{STD}(\tau)/Ca^*(\tau))$

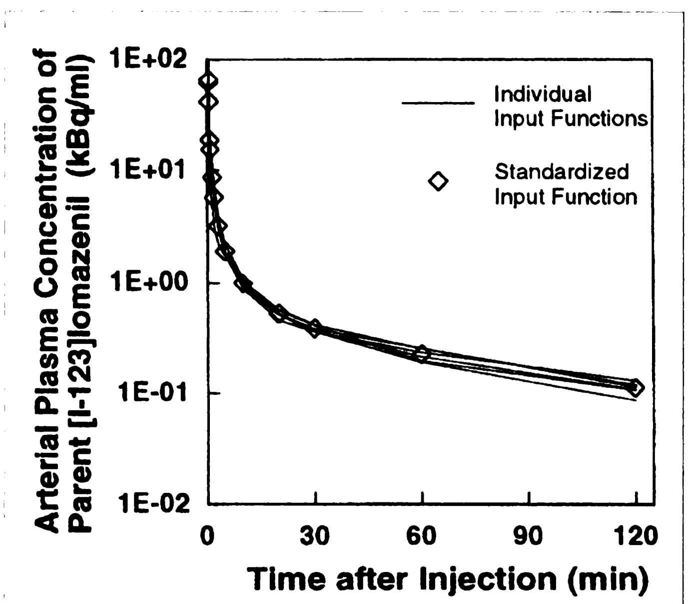

FIGURE 3. Actual arterial input functions in six subjects and the standardized input function. The radioactivity concentrations are corrected for physical decay and are normalized to an injected dose of 111 MBq. The standardized input function (y kBq/ml) is expressed as a function of time postinjection (t min) using a line (up-slope) and 5-exp (down-slope) as follows: $y = 0$ [$t < 0.38$]; $y = 655 \cdot (t - 0.38)$ [$0.38 < t < 0.54$]; $y = \Sigma A_i \cdot \exp(-\alpha_i \cdot (t - 0.54))$, where $A_1 = 76.5$, $A_2 = 23.6$, $A_3 = 3.74$, $A_4 = 0.717$, $A_5 = 0.239$, $\alpha_1 = 11.7$, $\alpha_2 = 1.54$, $\alpha_3 = 0.264$, $\alpha_4 = 0.0395$ and $\alpha_5 = 0.00638$ [$t > 0.54$].

TABLE 2
Mean Differences of the Areas under the Curve of Estimated Input Function from Those of Actual Input Function

Calibration time (min)	Difference from actual value (mean |%error|)			
	$\int_0^{10} Ca(t)\,dt$	$\int_0^{30} Ca(t)\,dt$	$\int_0^{60} Ca(t)\,dt$	$\int_0^{120} Ca(t)\,dt$
10	12.2%	8.9%	7.9%	7.9%
20	15.9%	12.6%	11.3%	11.1%
30	15.1%	11.8%	10.6%	10.4%
60	9.2%	8.1%	7.3%	6.3%
120	14.3%	12.3%	11.2%	10.2%

TABLE 3
Parameters of Blood Dynamics of Iodine-123-Iomazenil over Time

Time after injection (min)	AVR	PBR	LTR
3	1.302 ± 0.510	1.265 ± 0.100	0.572 ± 0.072
5	1.342 ± 0.316	1.476 ± 0.085	0.306 ± 0.057
10	1.172 ± 0.154	1.585 ± 0.072	0.164 ± 0.026
30	0.977 ± 0.027	1.587 ± 0.043	0.112 ± 0.011
60	0.911 ± 0.037	1.579 ± 0.061	0.102 ± 0.016
120	0.876 ± 0.030	1.526 ± 0.054	0.090 ± 0.018

The mean values ± s.d. in the six subjects are presented. AVR = arterial-to-venous ratio of the total radioactivity concentration in the whole blood; PBR = plasma-to-blood radioactivity concentration ratio in the arterial blood; LTR = lipophilic-to-total radioactivity concentration ratio in the arterial plasma.

and B_L/B_E were calculated from $C_{STD}(t)$ and sets of K_1 and k_3 (from 0.02 to 1.00 at 0.02 interval for both), then both parameters were determined from $B_E \cdot (C_{STD}(\tau)/Ca^*(\tau))$ and B_L/B_E by looking up the precalculated values (tables) with numerical interpolation. The former computation was carried out only once in the study because the same $C_{STD}(t)$ was used. The details in the implementation of the look-up tables have been described previously (*16*).

The estimated parameter obtained by this method were compared with the reference parameters described above.

RESULTS

The AIFs of each of the six subjects had similar shapes, and a SIF was successfully derived (Fig. 3). The error caused by variation in the shape of the input functions alone was minimal at a calibration time of 60 min postinjection (Table 2). The intersubject variation in AVR decreased with time and had a value near 1.0 at 30 min, and PBR and LTR showed less variability at 30 min or later (Table 3). Considering the above and some practical factors (discussed later), we chose 30 min postinjection as the time for calibration. Although the AVR was 0.977 at 30 min, it was considered that the arterial and venous blood were in a state of equilibrium and a value of 1.0 was used for AVR. The average values of PBR and LTR at 30 min were 1.587 and 0.112, respectively.

Figure 4 demonstrates the overall precision of the present method (using a single venous blood sample) with a calibration time of 30 min postinjection. The BP was estimated with an error of less than 10% in the cerebral cortical regions. The overall correlation coefficient was 0.941 ($p < 0.0001$), and the intrasubject correlation coefficients ranged from 0.992 to 0.997 ($p < 0.0001$ for all). K_1 showed relatively large errors (max. 30%), and the overall correlation was $r = 0.699$ ($p < 0.0001$). Within each subject, however, the correlation was excellent ($r = 0.916$ to 0.975; $p < 0.0001$ for all). The intercept by a regression analysis was not significant ($p = 0.073$ to 0.901), indicating that the estimates for each subject were on a line passing through the origin.

DISCUSSION

The present study demonstrated the feasibility and precision of a simplified method for quantification of benzodiazepine receptor binding using [^{123}I]iomazenil and SPECT. By using a SIF in conjunction with the table look-up procedure, the method required only a single venous blood sample without plasma separation or lipophilic extraction and two separate SPECT scans. These conditions may be practical in clinical settings. Overall, acceptable estimation of BP was possible, suggesting the validity of the present approach.

The error in the EIF-V is due to two factors, i.e., the error in the estimated scaling factor $Ca^*(\tau)$ and the variation in the shape of the input functions. The small intersubject variances of AVR, PBR and LTR observed at 30 min postinjection or later suggested the similarity of metabolism and excretion of iomazenil among the six subjects and supported the use of the total radioactivity concentration in the venous blood for the calibration instead of the arterial plasma lipophilic concentration in such a late phase.

Although calibration at 60 min postinjection showed minimal error arising from the latter factor, we chose 30 min as the calibration time for the following reasons:

1. Visual inspection of individual arterial curves suggested that one particular subject was primarily responsible for the time course of the error (data not shown), and the calibration time appeared to be arbitrary if the arterial lipophilic concentration could be accurately estimated.

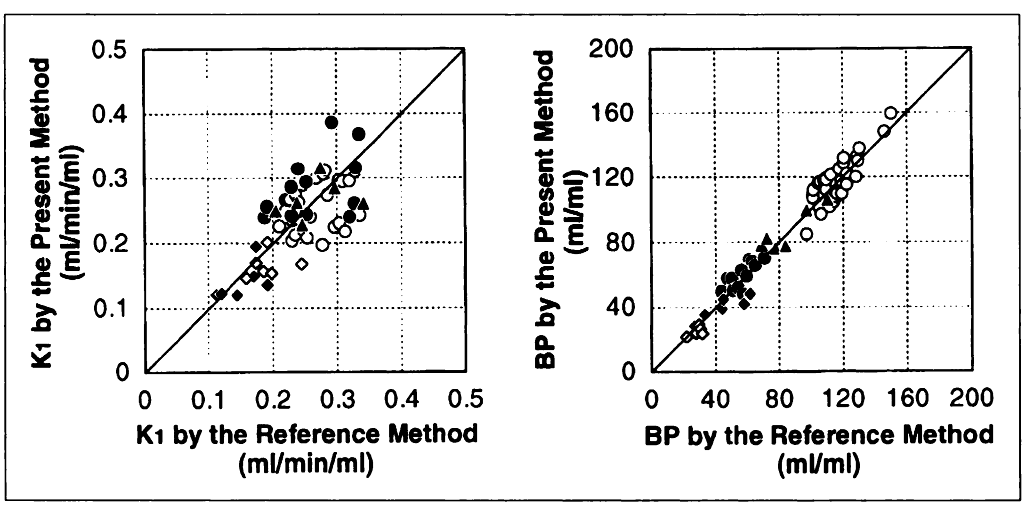

FIGURE 4. Correlation of K_1 (left) and BP (right) estimated by the present method (using venous blood sample) and by the reference curve-fitting method. A total of 60 ROIs from the six subjects were plotted. Open circles are cerebral cortex (n = 30); closed circles, the striatum and thalamus (n = 12); closed triangles, the cerebellum (n = 6); open diamonds, the pons (n = 6) and closed diamonds, white matter/ventricle (n = 6).

2. The appropriate time for estimating the arterial radioactivity concentration from the venous blood sample should be when the arterial and venous blood are in a state of equilibrium.
3. Thirty minutes postinjection would be optimal in clinical settings because blood sampling could be performed soon after the early SPECT acquisition.

Since the error in $Ca^*(\tau)$ is expected to influence the estimated K_1 and BP to the same degree, the much smaller error observed in the estimation of BP than of K_1 suggested the robustness of BP against the variation in the shape of the input function. In contrast, the K_1 estimation should be sensitive to errors in the integral amount of the input before the early scan. More precise estimation of K_1 could be achieved by more accurate estimation of the input in the early phase, that is, by an earlier calibration. The time course of AVR, however, indicated that the venous blood was not equilibrated with the arterial blood in such an early phase. Consequently, absolute estimation of K_1 with reasonable precision may not be possible when using venous blood samples. In terms of the intrasubject relative estimation, however, the reliability of K_1 was supported by the fact that the estimated values were well correlated with the reference values on the line passing through the origin.

The hematocrit value may have a significant effect on PBR, since the parent iomazenil appears to be diffusable and the metabolite not diffusable into blood cells (*24*). While no correlation was noted between the hematocrit values and PBRs in the present population, it should be further clarified whether considering the hematocrit value provides more accurate estimates of PBR in patients. Also, arterialized venous blood samples from a warmed hand, as have been used in quantitative FDG-PET (*20,25*) and IMP-SPECT studies (*26–28*), may allow earlier calibration and reduction of the error in $Ca^*(\tau)$, and thus has a potential for providing better precision. The applicability of this technique to iomazenil, a rapidly metabolized ligand, should be investigated.

Obviously, validation studies in other populations are indispensable. The data presented here were, however, rather uniform, suggesting applicability of the method to patients who have no liver or kidney complications and therefore metabolize and excrete iomazenil normally. It is expected that comparable input functions will be obtained in patients without such complications.

CONCLUSION

Absolute measurement of benzodiazepine receptor binding was possible with reasonable precision in normal humans by using a single venous blood sample and two separate SPECT scans with $[^{123}I]$iomazenil. The ligand transport (K_1) was also able to be estimated in terms of relative measurement. The present simplified method would be useful for quantitative assessment of benzodiazepine receptors in clinical settings.

REFERENCES

1. Höll K, Deisenhammer E, Dauth J, et al. Imaging benzodiazepine receptors in the human brain by single photon emission computed tomography (SPECT). *Nucl Med Biol* 1989;16:759–763.
2. Beer HF, Blauenstein PA, Hasler PH, et al. In vitro and in vivo evaluation of iodine-123-Ro 16-0154: a new imaging agent for SPECT investigations of benzodiazepine receptors. *J Nucl Med* 1990;31:1007–1014.
3. Johnson EW, Woods SW, Zoghbi S, et al. Receptor binding characterization of the benzodiazepine radioligand ^{125}I-Ro16-0154: potential probe for SPECT brain imaging. *Life Sci* 1990;47:1535–1546.
4. Innis R, Zoghbi S, Johnson E, et al. SPECT imaging of the benzodiazepine receptor in non-human primate brain with $[^{123}I]$Ro 16-0154. *Eur J Pharmacol* 1991;193:249–252.
5. Innis RB, Al-Tikriti MS, Zoghbi SS, et al. SPECT imaging of the benzodiazepine receptor: feasibility of in vivo potency measurements from stepwise displacement curves. *J Nucl Med* 1991;32:1754–1761.
6. Woods SW, Seibyl JP, Goddard AW, et al. Dynamic SPECT imaging of the benzodiazepine receptor in healthy human subjects with $[^{123}I]$Ro 16-0154. *Psych Res Neuroimaging* 1992;45:67–77.
7. van Huffelen AC, van Isselt JW, van Veelen CWM, et al. Identification of the side of the epileptic focus with ^{123}I-iomazenil SPECT. A comparison with ^{18}FDG-PET and ictal EEG findings in patients with medically intractable complex partial seizures. *Acta Neurochir (suppl)* 1990;50:95–99.
8. Ferstl FJ, Cordes M, Cordes I, et al. Iodine-123-iomazenil-SPECT in patients with focal epilepsies—a comparative study with ^{99m}Tc-HMPAO-SPECT, CT and MR. *Adv Exp Med Biol* 1991;287:405–412.
9. Schubiger PA, Hasler PH, Beer-Wohlfahrt H, et al. Evaluation of a multicenter study with iomazenil—a benzodiazepine receptor ligand. *Nucl Med Commun* 1991;12:569–582.
10. Cordes M, Henkes H, Ferstl F, et al. Evaluation of focal epilepsy: a SPECT scanning of ^{123}I-iomazenil versus HMPAO. *Am J Neuroradiol* 1992;13:249–253.
11. Haldemann RC, Bicik I, Pfeiffer A, et al. Iodine-123-iomazenil: a quantitative study of the central benzodiazepine receptor distribution. *Nucl Med* 1992;31:91–97.
12. Bartenstein P, Ludolph A, Schober O, et al. Benzodiazepine receptors and cerebral blood flow in partial epilepsy. *Eur J Nucl Med* 1991;18:111–118.
13. Laruelle M, Baldwin RM, Rattner Z, et al. SPECT quantification of $[^{123}I]$iomazenil binding to benzodiazepine receptors in nonhuman primates. I. Kinetic modeling of single bolus experiments. *J Cereb Blood Flow Metab* 1994;14:439–452.
14. Abi-Dargham A, Laruelle M, Seibyl J, et al. SPECT measurement of benzodiazepine receptors in human brain with $[^{123}I]$iomazenil: kinetic and equilibrium paradigms. *J Nucl Med* 1994;35:228–238.
15. Abi-Dargham A, Gandelman M, Zoghbi SS, et al. Reproducibility of SPECT measurement of benzodiazepine receptors in human brain with $[^{123}I]$iomazenil. *J Nucl Med* 1994;36:167–175.
16. Onishi Y, Yonekura Y, Mukai T, et al. Simple quantification of benzodiazepine receptor binding and ligand transport using $[^{123}I]$iomazenil and two SPECT scans. *J Nucl Med* 1995;36:1201–1210.
17. Koeppe RA, Holthoff VA, Frey KA, et al. Compartmental analysis of $[^{11}C]$flumazenil kinetics for the estimation of ligand transport rate and receptor distribution using positron emission tomography. *J Cereb Blood Flow Metab* 1991;11:735–744.
18. Holthoff VA, Koeppe RA, Frey KA, et al. Differentiation of radioligand delivery and binding in the brain: validation of a two-compartment model for $[^{11}C]$flumazenil. *J Cereb Blood Flow Metab* 1991;11:745–752.
19. Frey KA, Holthoff VA, Koeppe RA, et al. Parametric in vivo imaging of benzodiazepine receptor distribution in human brain. *Ann Neurol* 1991;30:663–672.
20. Takikawa S, Dhawan V, Spetseiris P, et al. Noninvasive quantitative fluorodeoxyglucose PET studies with an estimated input function derived from a population-based arterial blood curve. *Radiology* 1993;188:131–136.
21. Iida H, Itoh H, Bloomfield PM, et al. A method to quantitate cerebral blood flow using a rotating gamma camera and iodine-123-iodoamphetamine with one blood sampling. *Eur J Nucl Med* 1994;21:1072–1084.
22. Iida H, Itoh H, Nakazawa M, et al. Quantitative mapping of regional cerebral blood flow using iodine-123-IMP and SPECT. *J Nucl Med* 1994;35:2019–2030.
23. Mintun MA, Raichle ME, Kilbourn MR, et al. A quantitative model for the in vivo assessment of drug binding sites with positron emission tomography. *Ann Neurol* 1984;15:217–227.
24. Zoghbi SS, Baldwin RM, Seibyl JP, et al. Pharmacokinetics of the SPECT benzodiazepine receptor radioligand $[^{123}I]$iomazenil in human and nonhuman primates. *Nucl Med Biol* 1992;19:881–888.
25. Phelps ME, Huang SC, Hoffman EJ, Selin C, Sokoloff L, Kuhl DE. Tomographic measurement of local cerebral glucose metabolic rate in humans with $[^{18}F]$2-fluoro-2-deoxy-D-glucose: validation of method. *Ann Neurol* 1979;6:371–388.
26. Podreka I, Baumgartner C, Suess E, et al. Quantification of regional cerebral blood flow with IMP-SPECT. *Stroke* 1989;20:183–191.
27. Moriwaki H, Matsumoto M, Hashikawa K, et al. Quantitative assessment of cerebral blood flow by ^{123}I-IMP SPECT: venous sampling method with hand warming in the water bath. *Jpn J Nucl Med* 1993;30:481–488.
28. Ito H, Akaizawa T, Goto R, et al. A simple method for measurement of cerebral blood flow using ^{123}I-IMP SPECT with calibrated standard input function by one point blood sampling: validation of calibration by one point venous blood sampling as a substitute for arterial blood sampling. *Jpn J Nucl Med* 1994;31:1071–1076.